CHINESE JOURNAL OF GEOPHYSICS Vol.49, No.5, 2006, pp: 1210~1219

THIRTY-YEAR PERIOD IN SECULAR VARIATION OF THE MAIN GEOMAGNETIC FIELD

XU Wen-Yao[1] Henri-Claud Nataf[2] WEI Zi-Gang[1] DU Ai-Min[1]

1 *Institute of Geology and Geophysics, Chinese Academy of Sciences, Beijing* 100029*, China*

2 *Laboratoire de Geophysique Interne et Tectonophysique, Grenoble, France*

Abstract The main geomagnetic field, $\boldsymbol{B}$, and its secular variation, $\dot{\boldsymbol{B}}$, originate from the same dynamo process in the outer core. However, their spatial structure and temporal behaviors are drastically different. Using 'globally averaged unsigned annual rate', $\overline{\dot{X}}, \overline{\dot{Y}}, \overline{\dot{Z}}, \overline{\dot{H}}$ and $\overline{\dot{F}}$, to express the magnitude of the $\dot{\boldsymbol{B}}$-field, we studied periodicity of the $\dot{\boldsymbol{B}}$-field on the basis of IGRF-9 models. The results show that the $\dot{\boldsymbol{B}}$-field experienced a three-episode variation during the centennial period from 1900 to 2000. The maximum annual rates occurred respectively around 1910~1920, 1940~1950, and 1970~1980, showing a 30-year period. In addition, the rising phase in each episode is much shorter than the declining phase. The governing factor of this periodic variation is proved to be the non-dipole field (mainly the quatrupole field), instead of the dipole field, although the dipole field is dominative over all other multipoles in the main field $\boldsymbol{B}$.

Key words Main geomagnetic field, Secular variation, Dipole field, Non-dipole field, Unsigned annual rate

1 INTRODUCTION

The main geomagnetic field, $\boldsymbol{B}$, is subjected to changes in its direction, strength and spatial pattern on various timescales, known as secular variation (SV), $\dot{\boldsymbol{B}}(= \partial \boldsymbol{B}/\partial t)$. The $\boldsymbol{B}$ and $\dot{\boldsymbol{B}}$ originate from the same dynamo process in the outer core. However, their spatial structure and temporal behaviors are drastically different.

Among the verity of characteristics of the SV, periodic or cyclic features have long attracted studies. Different periods, ranging from years to millennia and even millions of years, have been revealed by the studies on paleomagnetism, archeomagnetism and historical data analysis.

Polarity reversal associated with the strength change has long, but irregular period, from tens of thousands to millions of years[1~3].

The dipole axis rotates around the geographic axis at a rate of about 0.05(°)/a, showing an 7000-year period. The non-dipole field drifts westward at a rate of 0.2(°)/a, and will take 1800 years for a complete round[4~9]. The variations of declination and inclination at London imply a period of some 600 years[10]. Long records of the geomagnetic field have been analyzed by using various spectrum techniques, such as Fourier analysis, wavelet analysis, Maximum Entropy Spectrum analysis (MESA), showing a well-known "century period" from 60 years to 100 years[11].

A typical short-period variation of the main field is geomagnetic jerk, which repeatedly occurs about every 10 years in twenty century. In addition, archeomagnetic jerks have been also examined[12].

Physical aspects of the periodicity in SV have been studied for a few decades. As widely accepted, the main field and its secular variations originate from fluid flow in the Earth's core. The flow pattern at the surface of the Earth's core can be deduced from the geomagnetic data observed at the Earth surface[13,14]. The knowledge about the fluid flow within the whole core, however, mainly relies on numerical MHD simulations[15~17].

The process and frequency of polarity reversals and associated variations of field strength depend not only on changes of the fluid flow in the core[15], but also on the thermal condition of the Earth's mantle and physical-chemical properties of the core-mantle boundary[18].

E-mail: wyxu@mail.igcas.ac.cn

Another important feature in the SV of the main field is westward drift of the non-dipole field. In order to understanding the westward drift, Jault et al.[19] examined the correlation of westward drift with exchanges of angular momentum between the core and the mantle. Hide[20] suggested a propagating magnetic mode of MHD wave in the outer core.

Studies of the main field and its secular variations strongly rely on a continuous long data series with proper accuracy. Unfortunately, this kind of data is now limited. The IGRF models supply a useful database, although it is too short. Using the method of Natural Orthogonal Components (NOC) to the IGRF models, Xu and Sun[21] analyzed the relationship between the variation periods of the main field and its special configuration, showing an interesting association of the eigenmodes (principal components) with special inherent periods. Similar time-space correlations have been found in other studies. For instance, Bellager et al.[22] correlated geomagnetic jerks with Changler wobble, whereas Bloxham et al.[23] show that geomagnetic jerks can be explained by the combination of a steady flow and a simple time-varying axisymmetric, equatorial symmetric toroidal zonal flow.

Previous studies are mostly interested in characteristics of the main field $\boldsymbol{B}$ and its evolution. In this paper we focus on periodical characteristics of the $\dot{\boldsymbol{B}}$ field. The 9-th generation of IGRF[24,25] is used to study evolution of the secular variation in the main field for recent 100 years.

2 EVOLUTION OF THE SV-FIELD

The potential of the main geomagnetic field is conventionally represented by spherical harmonic series as follows

$$V(r,\theta,\lambda) = a\sum_{n=1}^{N}\sum_{m=0}^{n}\left(\frac{a}{r}\right)^{n+1}(g_n^m\cos m\lambda + h_n^m\sin m\lambda)P_n^m(\theta). \tag{1}$$

In this series, the first 3 terms with degree $n=1$ describe the dipole (briefly, DP) part in the main field. The following terms with $n \geq 2$ represent the non-dipole part (ND), among which the 5 terms with $n=2$ represent a quadrupole field, and the 7 terms with $n=3$ for a octapole field. The power of the geomagnetic field of degree n on the Earth's surface may be written in terms of Gauss coefficients g_n^m and h_n^m as follows[5,26]

$$R_n = (n+1)\sum_{m=0}^{n}[(g_n^m)^2 + (h_n^m)^2], \tag{2}$$

$R_n(n)$, usually called 'geomagnetic spectrum', is a function describing the distribution of the power with respect to degree n. In this paper the function $R_n(n)$ is named as 'Main field-spectrum' or '$\boldsymbol{B}$-spectrum' in order to distinguish from the spectrum of the SV-field (or $\dot{\boldsymbol{B}}$-spectrum) and the quasi spectrum of the SV-field (or $\boldsymbol{Q}\dot{\boldsymbol{B}}$-spectrum), which will be introduced in following discussion.

Figure 1a shows the $\boldsymbol{B}$-spectra R_n for every 5 years during the period from 1900 to 2000 by 21 curves. It is noted that the power R_1 of the dipole field is obviously dominant over other multipoles $R_n(n=2,3,\cdots)$, making the geomagnetic field pattern look like a dipole field.

The SV-field is the first time-derivative of the main field, $\dot{\boldsymbol{B}}(=\partial\boldsymbol{B}/\partial t)$, usually represented by annual rate of the field. The power spectrum of the $\dot{\boldsymbol{B}}$-field, referred to as 'SV spectrum', or '$\dot{\boldsymbol{B}}$-spectrum', can be deduced from formula (2)

$$\dot{R}_n = 2(n+1)\sum_{m=0}^{n}[g_n^m\dot{g}_n^m + h_n^m\dot{h}_n^m], \tag{3}$$

where $\dot{g}_n^m$ and $\dot{h}_n^m$ are the first time-derivative (or annual rate) of the Gauss coefficients g_n^m and h_n^m. Regardless of sigh, the Gauss coefficients of the dipole field, mainly g_1^0, are much greater than all other coefficients in high-degree multipoles. Therefore, even a small annual rate $\dot{g}_1^0$ will leads to a great magnitude of $\dot{R}_1$. In other words, the dipole field is always dominant in the $\dot{\boldsymbol{B}}$-spectrum, just as the dipole field does in the $\boldsymbol{B}$-spectrum. Fig. 1b illustrates the $\dot{\boldsymbol{B}}$-spectrum, regardless of sigh of $\dot{R}_n$, clearly showing a similar trend as those in Fig. 1a. Fig. 1c shows time-variations of the annual rates $\dot{R}_n$ for $n = 1\sim 5$. The large negative values of $\dot{R}_1(-1\times 10^6 \sim$

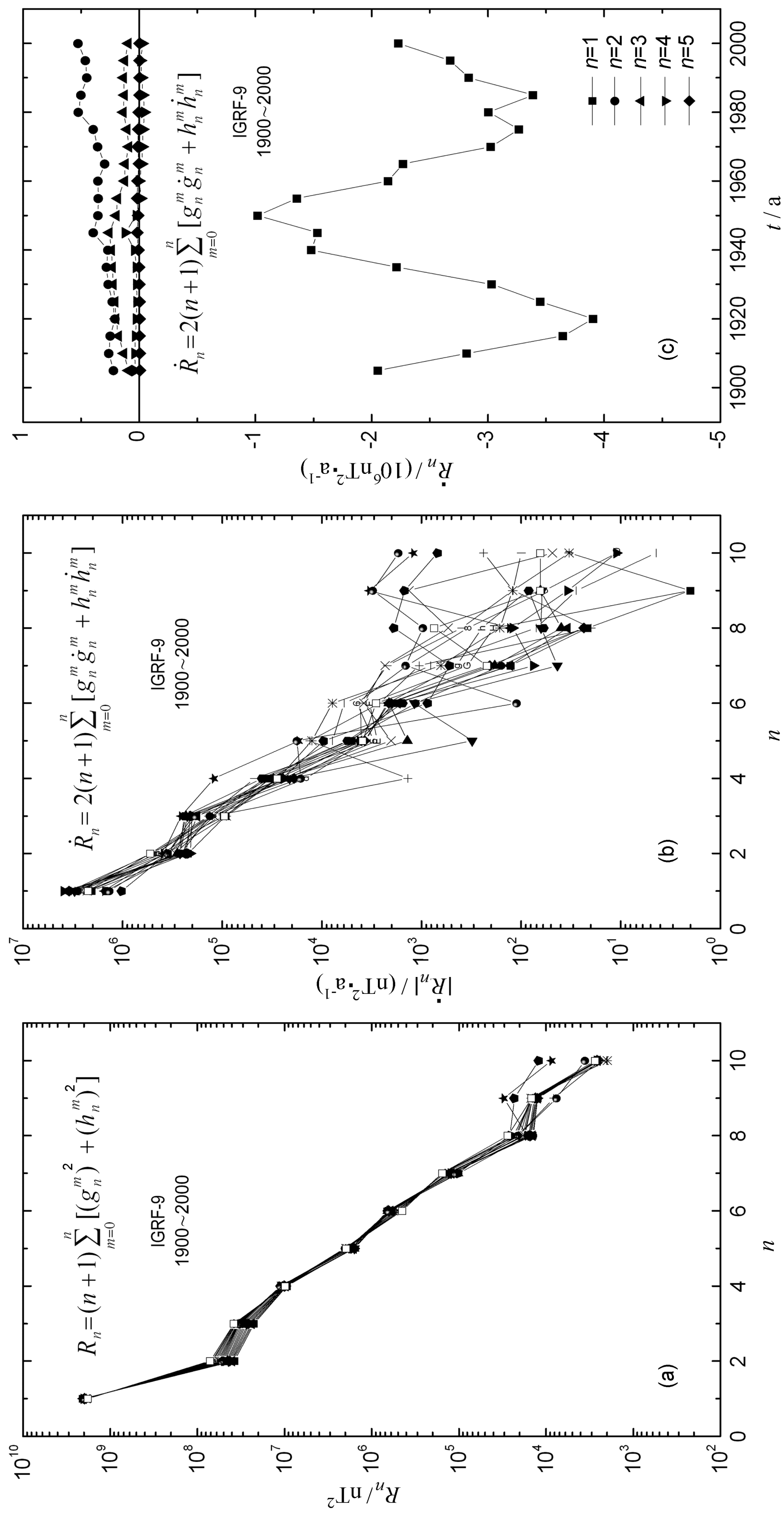

Fig.1 Geomagnetic spectrum and its variation rate

(a) The **B**-field spectrum R_n (n=1~10); (b) The annual rate $\dot{R}_n$ (n=1~10); (c) Time variations of $\dot{R}_n$ (n=1~5).

$4\times10^6\text{nT}^2/\text{a}$) mean a steady decrease of the dipole field, whereas the relatively small positive $\dot{R}_n$ (generally, $< 0.5\times10^6\text{nT}^2/\text{a}$ for $n = 2\sim5$) represent minor enhancements of the multipole fields.

The above-mentioned features of the $\dot{\boldsymbol{B}}$ field may mislead to an incorrect conclusion: the spatial distribution of the annual rate (or the pattern of the SV-field $\dot{\boldsymbol{B}}$) is also controlled by the dipole field.

In fact, the SV-field pattern is dependent on $\dot{g}_n^m$ and $\dot{h}_n^m$, instead of g_n^m, h_n^m and $\dot{R}_n$. Comparing the annual rates of the Gauss coefficients of the dipole field ($\dot{g}_1^0, \dot{g}_1^1$ and $\dot{h}_1^1$) with other $\dot{g}_n^m$ and $\dot{h}_n^m$ for $n\geq 2$, we found no essential difference between them, as shown in Fig. 2.

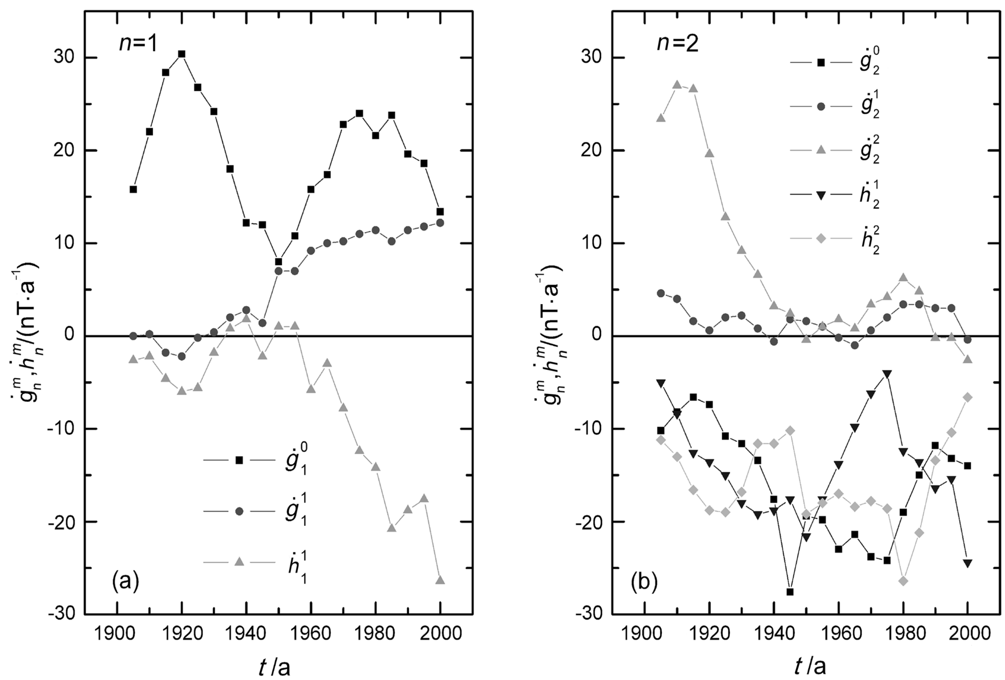

Fig. 2 Comparison of annual rates of Gauss coefficients in the main geomagnetic field

(a) For dipole; (b) For quatrupole.

Using two successive IGRF models for epochs t_1 and t_2, one can obtain the average annual rate of the main field during this time span. Fig. 3 shows the SV-field of Z component calculated for several 5-year intervals. It is noted in the figure that the most important features of the SV-field are several local regions with remarkable annual rate, instead of global decrease, as suggested by the dipole moment decline. This fact implies the leading role of the non-dipole field in the SV-field.

Since the number of Gauss coefficients for a special degree n is $2n+1$, the contribution of a multipole with degree n to the main field is a comprehensive exhibition of all coefficients included in this multipole. Following the idea of $\boldsymbol{B}$-spectrum in Eq.(2) and replacing g_n^m and h_n^m with $\dot{g}_n^m$ and $\dot{h}_n^m$, we define a 'Quasi spectrum of the SV-field' (or briefly, $\boldsymbol{Q}\dot{\boldsymbol{B}}$-spectrum) as follows

$$W_n = (n+1)\sum_{m=0}^{n}[(\dot{g}_n^m)^2 + (\dot{h}_n^m)^2]. \tag{4}$$

Figure 4 depicts the $\boldsymbol{Q}\dot{\boldsymbol{B}}$-spectra for every 5 years during 1900~2000. It is noted in the figure that the quadrupole is dominant in the $\boldsymbol{Q}\dot{\boldsymbol{B}}$-spectrum, showing a different feature from the $\dot{\boldsymbol{B}}$-spectrum,.

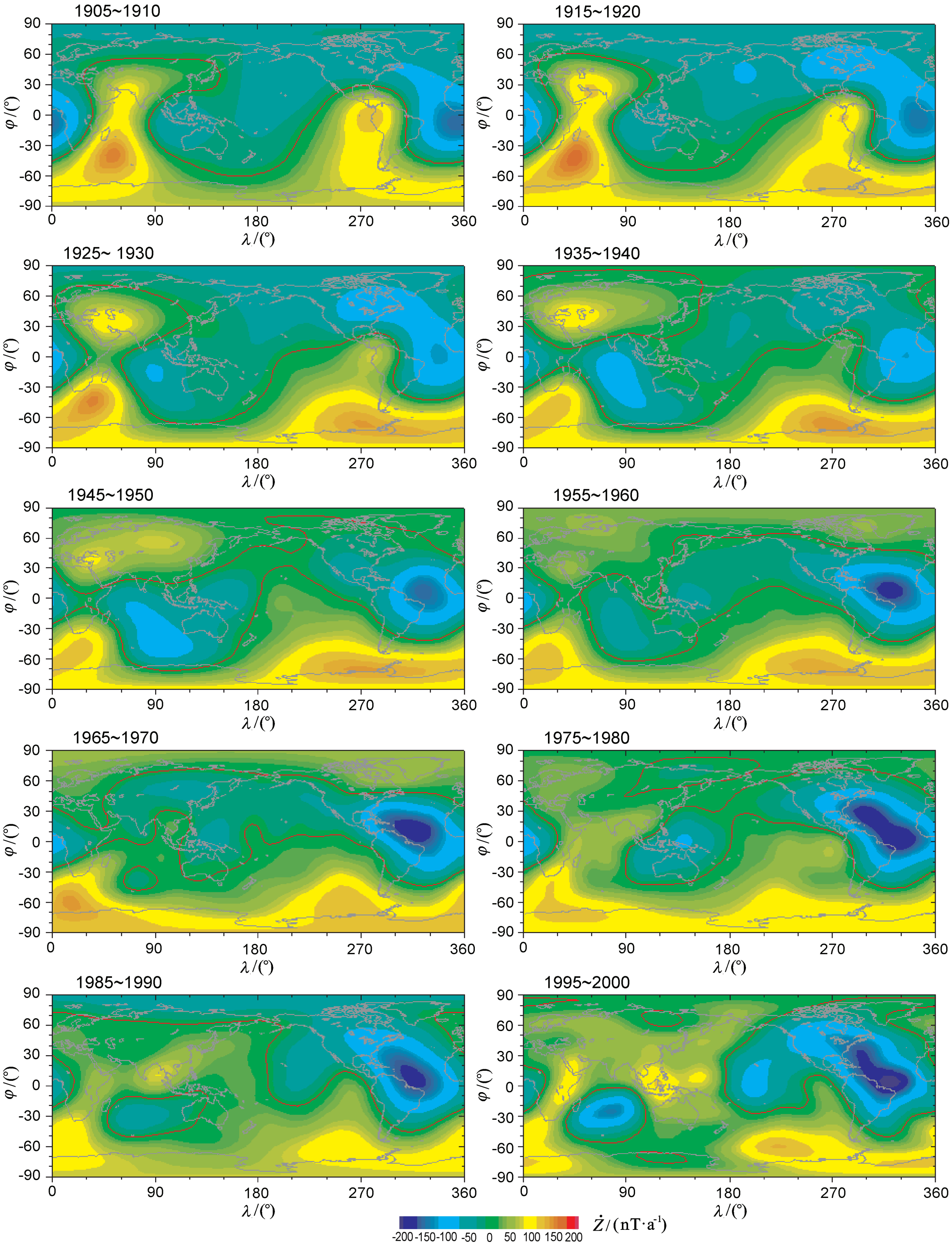

Fig. 3 Secular variation (SV-field) of Z component

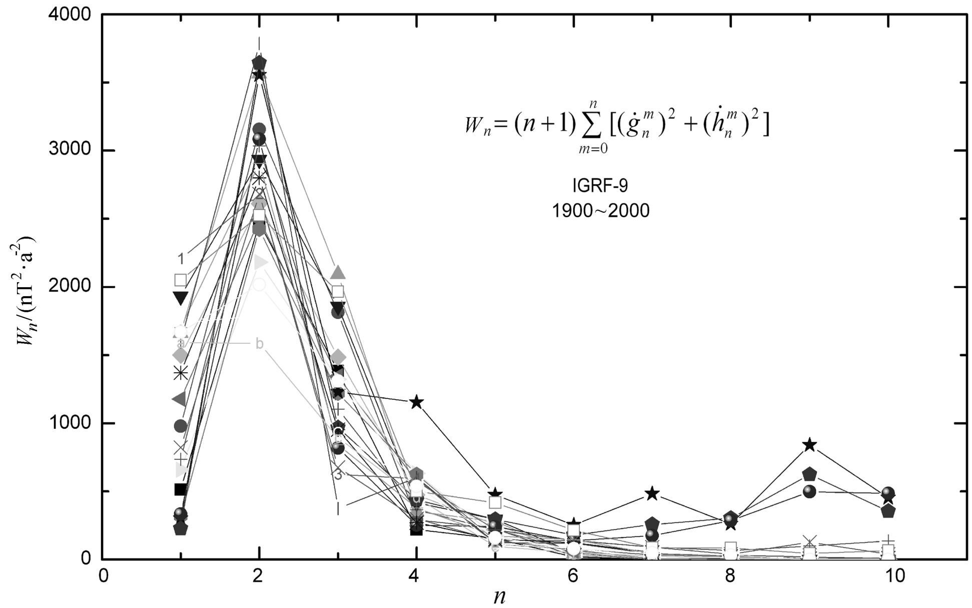

Fig. 4 Quasi spectrum of the SV-field

The main purpose of this paper is to study the overall features of the global SV-field, instead of its detailed spatial distribution. Therefore, it is necessary to choose a proper measure for this description. As discussed above, the dipole moment is obviously not a suitable quantity for describing the SV-field. The maximum value of the field is also not suitable, since this value is for only one position, instead of for the whole globe. The global average value of the field seems to be a better choice.

Bondi and Gold[27] elucidated a quantity, pole-strength, as an useful measure of the strength of an internally generated magnetic field

$$P(S,t) = \iint_s |\boldsymbol{B}\cdot\hat{\boldsymbol{n}}|\mathrm{d}S,$$

where S is a closed surface surrounding the magnetic sources, such as the surface of a planet, $\hat{\boldsymbol{n}}$ is the outward unit vector of the surface, $\boldsymbol{B}$ the magnetic field at the surface. This quantity, later called "unsigned magnetic flux", is widely used in geomagnetism[28~33]. Since the contributions from both the dipole and the multipoles are included, the pole-strength is an adequate measure for describing the global features of the field, in comparison with the dipole moment and the maximum field strength.

Following this idea, we define a globally averaged unsigned annual rate of Z component as follows

$$\overline{\dot{Z}} = \frac{1}{S}\int_o^{\pi}\int_0^{2\pi}|\dot{Z}|r^2\sin\theta\mathrm{d}\lambda\mathrm{d}\theta, \tag{5}$$

where θ and λ are colatitude and longitude, respectively. $\dot{Z}$ represents the annual rate of Z component at the position (θ,λ). Similarly, we have $\overline{\dot{X}}, \overline{\dot{Y}}, \overline{\dot{H}}$ and $\overline{\dot{F}}$ for northward, eastward and horizontal components, as well as total intensity.

In this paper the 9-generation of IGRF, which includes 21 main field models for every 5 years from 1900 to 2000 and one secular variation model for 2000~2005, is used to calculate the SV-field. Fig. 5 shows the

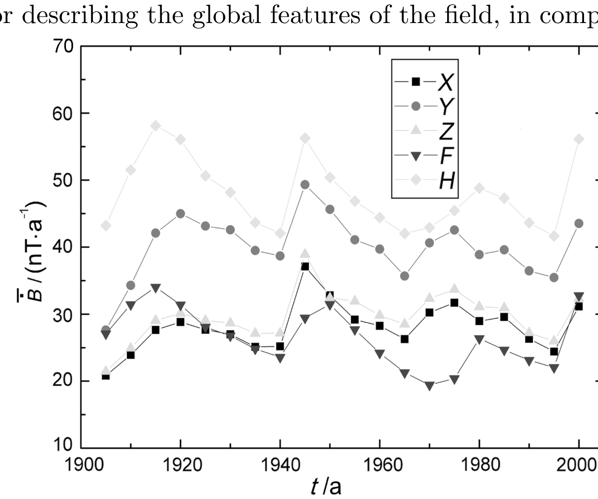

Fig. 5 Variations of the globally averaged unsigned annual rates $\overline{\dot{X}}, \overline{\dot{Y}}, \overline{\dot{Z}}, \overline{\dot{H}}$ and $\overline{\dot{F}}$

variations of the globally averaged unsigned annual rates of 5 elements X, Y, Z, H and F. It is interesting to note that the annual rates of these components consistently show a fairly regular oscillation variation. During the centennial period from 1900 to 2000, the secular variation of the main field experienced a three-episode variation. The maximum annual rates of these elements consistently occurred around 1910~1920, 1940~1950, and 1970~1980, showing a 30-year period variation. In addition, the rising phase in each episode is much shorter than declining phase. The detail information of the annual rates are listed in Table 1.

Table 1 Characteristics of the main field secular variation for 1900~2000

	Mean ($nT\cdot a^{-1}$)	Max.($nT\cdot a^{-1}$)	Min.($nT\cdot a^{-1}$)	Range($nT\cdot a^{-1}$)	1-st peak t_{max1}	2-nd peak t_{max2}	3-rd peak t_{max3}
$\dot{X}$	29.6	38.9	21.4	17.5	1915~1920	1940~1945	1970~1975
$\dot{Y}$	26.5	34.0	19.4	14.6	1910~1915	1945~1950	1975~1980
$\dot{Z}$	48.0	58.1	41.7	16.5	1910~1915	1940~1945	1975~1980
$\dot{H}$	28.1	37.1	20.8	16.3	1915~1920	1940~1945	1970~1975
$\dot{F}$	40.1	49.3	27.6	21.7	1915~1920	1940~1945	1970~1975
Average					1910~1920	1940~1950	1970~1980

3 ORIGIN OF THE PERIODIC VARIATION IN THE SV-FIELD

As well known, the most prominent feature in the secular variation of the main field is steady decrease of the dipole moment. Let us examine first if the dipole moment variation can explain the periodic trends of the $\dot{\boldsymbol{B}}$-field shown in Fig. 5 and Table 1.

Figure 6a and 6b illustrate the steady decrease tendency of the dipole moment M_{DP} and the time-variation of its annual rate $\dot{M}_{DP}$ for the period 1900~2000. It is noted that the magnitude of the annual rate of the dipole moment, $|\dot{M}_{DP}|$, reaches the maxima around 1930 and 1980, while there is a minimum around 1950. This variation implies that the 1950' peak in Fig. 5 and Table 1 is hard to be explained by the dipole field variation, even though the 1920' and 1980's peaks might be attributed to the dipole field. In fact, even the 1920' and 1980's peaks are mainly caused by the non-dipole field, that will be shown in the following discussion.

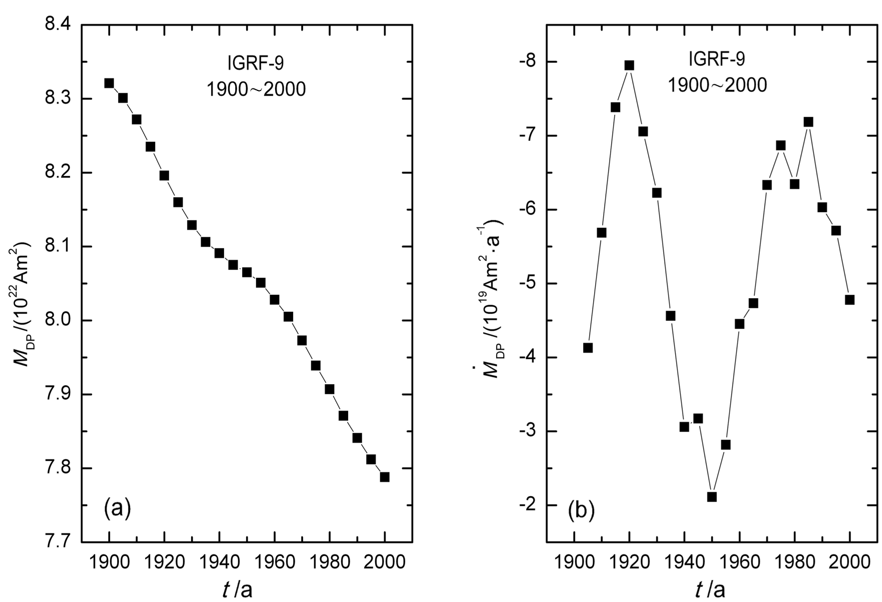

Fig. 6 Time-variations of the dipole moment (a) and its annual rate (b)

In order to determine the principal contributor to the $\dot{\boldsymbol{B}}$-field, we calculated the total SV-fields $\dot{\boldsymbol{B}}_{TT}$ and the parts caused by the dipole field ($\dot{\boldsymbol{B}}_{DP}$) and non-dipole field ($\dot{\boldsymbol{B}}_{ND}$). As an example, Fig. 7 illustrates the

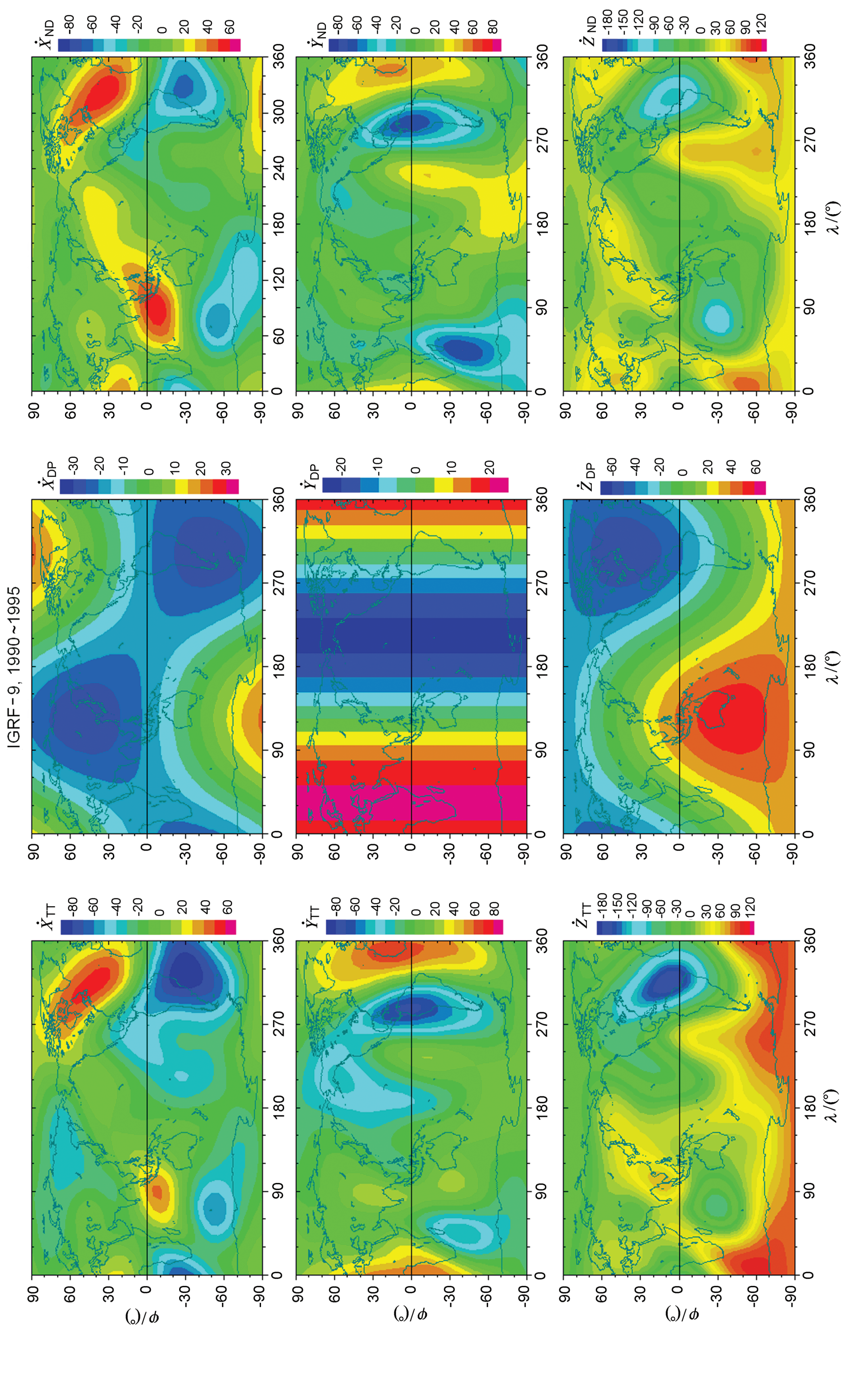

Fig. 7 Global distributions of the annual rate for 1990~1995

global distributions of $\dot{\boldsymbol{B}}_{\mathrm{TT}}, \dot{\boldsymbol{B}}_{\mathrm{DP}}$, and $\dot{\boldsymbol{B}}_{\mathrm{ND}}$ for three components X, Y, and Z. The left column in Fig. 7 is for $\dot{X}_{\mathrm{TT}}, \dot{Y}_{\mathrm{TT}}$, and $\dot{Z}_{\mathrm{TT}}$, the middle column for $\dot{X}_{\mathrm{DP}}, \dot{Y}_{\mathrm{DP}}$, and $\dot{Z}_{\mathrm{ND}}$, and the right column is for $\dot{X}_{\mathrm{ND}}, \dot{Y}_{\mathrm{ND}}$, and $\dot{Z}_{\mathrm{ND}}$. It is noted that the overall features of the $\dot{\boldsymbol{B}}_{\mathrm{TT}}$ are generally similar to those for the $\dot{\boldsymbol{B}}_{\mathrm{ND}}$ in both pattern and intensity, suggesting that the SV-field is mainly governed by the non-dipole field $\dot{\boldsymbol{B}}_{\mathrm{ND}}$.

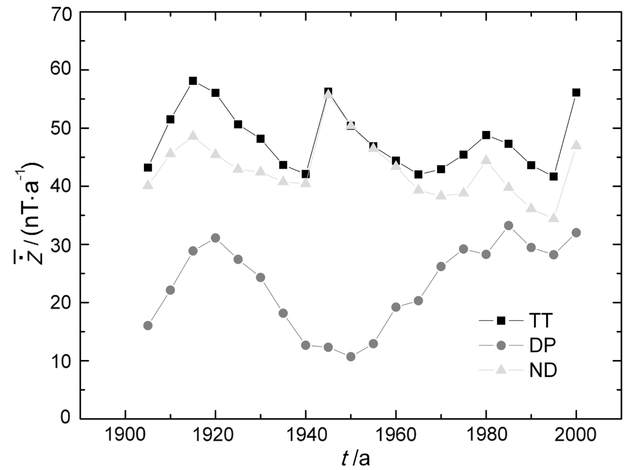

Fig. 8 Globally averaged unsigned annual rates of the dipole, non-dipole and total field for Z component

Figure 8 shows the unsigned average annual rates of the Z component for the dipole field ($\overline{\dot{Z}}_{\mathrm{DP}}$), non-dipole field ($\overline{\dot{Z}}_{\mathrm{ND}}$), and the whole field ($\overline{\dot{Z}}_{\mathrm{TT}}$). In general, $\overline{\dot{Z}}_{\mathrm{ND}}$ is about twice of $\overline{\dot{Z}}_{\mathrm{DP}}$, suggesting that the SV-field is mainly governed by the non-dipole field $\dot{B}_{\mathrm{ND}}$. Around the 1950' peak, the rate is about 55 nT/a, much greater than the rate $\overline{\dot{Z}}_{\mathrm{DP}}$ (10 nT/a), showing a dominant role to the total rate. As for 1920' and 1980' peaks, the rate $\overline{\dot{Z}}_{\mathrm{DP}}$ reaches its maximum, although it is less than the rate $\overline{\dot{Z}}_{\mathrm{ND}}$.

4 SUMMARY

(1) During the centennial period from 1900 to 2000, the secular variation of the main geomagnetic field experienced a three-episode variation. The maximum annual rates occurred respectively around 1910~1920, 1940~1950, and 1970~1980, showing a 30-year period. In addition, the rising phase in each episode is much shorter than declining phase.

(2) Comparison of the dipole and non-dipole fields shows that the non-dipole field is dominant in the SV-field ($\dot{\boldsymbol{B}}$-field). This feature is different from the main field ($\boldsymbol{B}$-field).

(3) The governing factor of 30-year periodic variation in the SV field is the non-dipole field. The contribution of the non-dipole field to the SV field is about twice of the dipole field.

ACKNOWLEDGMENTS

This work was supported by the National Natural Science Foundation of China (40436016).

REFERENCES

[1] Merrill R T, McFadden P L. Geomagnetic polarity transitions. *Rev. Geophys.*, 1999, **37**(2): 201~226

[2] Guyodo Y, Valet J P. Global changes in intensity of the Earth's magnetic field during the past 800 kyr. *Nature*, 1999, **399**: 249~252

[3] Valet J P. Time variations in geomagnetic intensity. *Rev. Geophys.*, 2003, **41**(1): 4-1~4-43

[4] Malin S R C, Saunders I. Rotation of the Earth's magnetic field. *Nature*, 1973, 245~246

[5] Langel R A. The Main Field. In: Jacobs J A, ed. Geomagnetism, Vol 1. London: Academic Press, 1987. 249~512

[6] Wei Z Gang, Xu W Y. Westward drift of the geomagnetic anomaly in East Asia. *Chinese J. Geophys.* (in Chinese), 2000, **43**(1): 49~56

[7] Wei Z G, Xu W Y. Drift and intensity variations of the geomagnetic field. *Chinese J. Geophys.* (in Chinese), 2001, **44**(4): 500~509

[8] Wei Zi-Gang, Xu Wen-Yao. Latitudinal dependence of westward drift of the geomagnetic field and its dispersion. *Chinese Sci. Bull.*, 2002, **47**(4): 330~333

[9] Wei Zi-Gang , Xu Wen-Yao. Westward drift in secular variation of the geomagnetic field. *Earth Planets Space*, 2003, **55**(3): 131~137

[10] Chapman S, Bartels J. Geomagnetism. London: Oxford University Press, 1940

[11] Wang D I, Sun W, Tschu K K. A note on MESA and spectral analysis of the Hundred-year geomagnetic data at Zo-Se. *Geophys. J. R. Astr. Soc.*, 1982, **71**: 275∼283

[12] Gallet Y, Genevey A, Courtillot V. On possible occurrence of 'archaeomagnetic jerks' in the geomagnetic field over the past three millennia. *Earth Plan. Sci. Lett.*, 2003, **214**: 237∼242

[13] Gubbins D. Finding core motions from magnetic observations. *Philos. Trans. R. Soc. London*, Ser.A, 1982, **306**(1): 247∼256

[14] Bloxham J, Jackson A. Fluid flow near the surface of Earth's outer core. *Rev. Geophys.*, 1991, **29**(1): 97∼120

[15] Glatzmair G A, Roberts P H. A three-dimensional self-consistent computer simulation of geomagnetic field reversal. *Nature*, 1995, **377**: 203∼209

[16] Kuang W, Bloxham J. An earth-like numerical dynamo model. *Nature*, 1997, **389**: 371∼374

[17] Kono M, Roberts P H. Recent geodynamo simulations and observations of the geomagnetic field. *Rev. Geophys.*, 2002, **40**(1): 4-1∼4-53

[18] Glatzmaier G A, Coe R S, Hongre L, et al. The role of the Earth's mantle in controlling the frequency of geomagnetic reversals. *Nature*, 1999, **401**: 885∼890

[19] Jault D, Gire C, Le Mouel J L. Westward drift, core motions and exchanges of angular momentum between core and mantle. *Nature*, 1988, **336**: 353∼356

[20] Hide R. How to locate the electrically conducting fluid core of a planet from external magnetic observations. *Nature*, 1978, **271**: 640∼641

[21] Xu W Y, Sun W. Eigen mode analysis of the Earth's main magnetic field during 1900∼2000. *Chinese J. Geophys.* (in Chinese), 1998, **41**(2): 187∼196

[22] Bellager E, Le Mouel J L, Mandea M et al. Changler wobble and geomagnetic jerks. *Phys. Earth Plan. Int.*, 2001, **124**: 95∼103

[23] Bloxham J, Zatman S, Dumberry M. The origin of geomagnetic jerks. *Nature*, 2002, **420**: 65∼68

[24] IAGA Division 5, Working Group 8. International geomagnetic reference field 2000. *Geophys. J. Int.*, 2000, **141**(1): 259∼262

[25] IAGA Division 5, Working Group 8. The 9-th generation International geomagnetic reference field. *Geophys. J. Int.*, 2003, **155**(18): 1051∼1056

[26] Lowes F J. Spatial power spectrum of the main geomagnetic field, and extrapolation to the core. *Geophys. J. R. Astron. Soc.*, 1974, **36**: 717∼730

[27] Bondi H, Gold T. On the generation of magnetism by fluid motion. *Mon. Not. R. Astro. Soc.*, 1950, **110**: 607∼611

[28] Roberts P H, Scott S. On analysis of the secular variation. 1. A hydromagnetic constraints: theory. *J. Geomag. Geoelectr.*, 1965, **17**(2): 137∼151

[29] Hide R, Malin S R C. On the determination of the size of the Earth's core from observations of the magnetic secular variation. *Proc. R. Soc. London*, Ser. A, 1981, **378**(1): 15∼33

[30] Li K, Xu W Y, Tschu K K. On the determination of radius and velocities of the Earth core by means of geomagnetic data. *Chinese J. Geophys.* (in Chinese), 1986, **29**(2): 117∼123

[31] Benton E R, Estes R H, Langel R A. Geomagnetic field modelling incorporating constraints from frozen-flux electromagnetism. *Phys. Earth Plan. Int.*, 1987, **48**(3-4): 241∼264

[32] Voorhies C V, Benton E R. Pole-strength of the Earth from MAGSAT and magnetic determination of the core radius. *Geophys. Res. Lett.*, 1982, **9**(4): 258∼261

[33] Xu W Y. Secular variations of the planetary-scale geomagnetic anomalies. *Chinese J. Geophys.* (in Chinese), 2001, **44**(2): 177∼186